Z. Physik A 281, 189–197 (1977)

Zeitschrift
für Physik A

Stark Interaction for Excited States in Alkali Atoms, Investigated by Laser Spectroscopy

K. Fredriksson and S. Svanberg
Department of Physics, Chalmers University of Technology, Göteborg, Sweden

Received January 14, 1977

The scalar polarizability constant α_0 for excited S- and D-states in rubidium and cesium was measured utilizing a two-step excitation scheme. An rf lamp and a single-mode dye laser were used to excite the atoms in a collimated atomic beam. Values of α_0 were determined for the 9–10 $^2S_{1/2}$ and 7–8 $^2D_{3/2}$ states of rubidium and for the 10–13 $^2S_{1/2}$, 9–10 $^2D_{3/2}$ and 9–11 $^2D_{5/2}$ states of cesium. Further, the isotope shift was evaluated in the 5579 Å rubidium line. A review of experimental polarizability constants for rubidium and cesium is given, and the results are compared with theoretical values.

1. Introduction

When an electric field is applied to an atom, the energy levels of the atom will be shifted. The shift has a quadratic dependence on the electric field for all atoms with no degeneracy with regard to the orbital quantum number l. This so called Stark effect is caused by a coupling between states that are connected by electric dipole transitions. For a moderately large perturbation the Stark shift can mathematically be described in terms of a scalar polarizability α_0 and a tensor polarizability α_2, according to the following formula:

$$\Delta E_s = -\tfrac{1}{2}\left[\alpha_0 + \alpha_2 \frac{3m_J^2 - J(J+1)}{J(2J-1)}\right]\mathcal{E}^2 \qquad (1)$$

valid for an atom in the sublevel m_J of an atomic state J in a uniform electric field $\mathcal{E}$. Whereas α_0 describes equal shifts for all the sublevels of a state, the term with α_2 also gives a splitting of sublevels, depending on $|m_J|$. By measuring the splittings of the sublevels in a level-crossing experiment, or by using quantum-beat spectroscopy, the tensor polarizability α_2 can be determined. Using these techniques, α_2-parameters of several P and D states in the alkali atoms have been measured [1–4, and ref. therein]. However, the determination of the scalar polarizability requires a method for measuring the absolute wavelength shift due to the application of the electric field. As this change is caused by the Stark effect of the two states involved in the transition, only the difference between the α_0 parameters for the two states can be measured. The tensor polarizability α_2 can also be obtained in such measurements of wavelength shifts.

In this work we have used step-wise excitations to study S and D states of rubidium and cesium. To obtain a high spectral resolution we reduced the line widths of the studied transitions by using a single-mode dye-laser beam, incident at right angles to a collimated atomic beam. The atoms were excited by the laser from the lowest P states, that were populated using an rf lamp. Measurements of the α_0 parameters for four states in rubidium and nine states in Cs are presented in this paper. Three of these values were reported in a previous letter [5]. The used measuring method was to Stark-scan the atomic sublevels to resonance with the dye-laser frequency, which was set slightly off the field-free resonance value. The fulfilled resonance condition was manifested by the occurance of fluorescent light. By combining information on α_0 and α_2 for the same states, oscillator strengths for transitions between the studied and close-lying states can be obtained. Certain difficulties in doing this for heavy alkali atoms are pointed out in this paper.

Another method of obtaining the scalar and tensor polarizabilities has been used by Harvey et al. [6]. Employing the Doppler-free two-photon spectro-

scopy method, the Stark effect of the $5s$ and $4d$ levels of sodium was studied. Very recently this technique has been extended to higher-lying sodium states [7], taking advantage of the resonant enhancement of the two-photon absorption cross-section possible when using two lasers with different frequencies.

2. Theory of the Stark Effect

The influence of an electric field on the energy states of an atom has been studied theoretically by, among others, Khadjavi et al. [8]. The perturbation of the states by an electric field $\mathcal{E}$ is described by the operator $-\mathcal{E}\cdot\mathbf{p}$, where $\mathbf{p}=-\sum_i e\cdot\mathbf{r}_i$ is the electric dipole moment of the atom. In the case of a weak electric field, J, describing the electronic angular momentum, can be treated as a good quantum number. The matrix elements of the Stark operator will differ from zero only between states of opposite parity, from which it follows, that there will be no first-order contribution to the energy. The second-order contribution is:

$$\Delta E(J,m) = \sum_{\gamma' J' m'} \frac{\langle \gamma J m|\,\mathcal{E}\cdot\mathbf{p}\,|\gamma' J' m'\rangle\langle\gamma' J' m'|\,\mathcal{E}\cdot\mathbf{p}\,|\gamma J m\rangle}{E(\gamma J)-E(\gamma' J')} \tag{2}$$

where $\langle\gamma J m|$ is the studied state and the sum is extended over all states connected to the studied state by electric dipole transitions. This sum can be expressed as the first order contribution of an effective operator,

$$H' = \sum_{\gamma' J' m'} \frac{\mathcal{E}\cdot\mathbf{p}\,|\gamma' J' m'\rangle\langle\gamma' J' m'|\,\mathcal{E}\cdot\mathbf{p}}{E(\gamma J)-E(\gamma' J')}. \tag{3}$$

By expanding H' in terms of irreducible spherical tensors, one can show [8], that H' consists of just two terms according to the simple formula:

$$H' = -\tfrac{1}{2}\alpha_0\,\mathcal{E}^2 - \tfrac{1}{2}\alpha_2\,\mathcal{E}^2\,\frac{3J_z^2-J(J+1)}{J(2J-1)}, \tag{4}$$

where α_0 and α_2 are the scalar and tensor polarizabilities, respectively. The electric field $\mathcal{E}$ is applied along the z axis. From this equation the energy shifts are then obtained, as given by Equation (1).

The values of α_0 and α_2 are determined by the squares of the reduced matrix elements of the electric dipole moment, $(J\|\,p\,\|J')^2$, but can as well be expressed in terms of the oscillator strengths $f_{\gamma L\to\gamma' L'}$ between the studied state and the interacting states. In terms of the reduced matrix elements we have:

$$\alpha_0 = -\tfrac{2}{3}\sum_{\gamma' J'} \frac{|(\gamma J\|\,p\,\|\gamma' J')|^2}{(2J+1)(E(\gamma J)-E(\gamma' J'))} \tag{5}$$

and

$$\alpha_2 = 2\left(\frac{10J(2J-1)}{3(2J+3)(J+1)(2J+1)}\right)^{1/2}\sum_{\gamma' J'}\frac{|(\gamma J\|\,p\,\|\gamma' J')|^2}{E(\gamma J)-E(\gamma' J')} \cdot(-1)^{J+J'+1}\begin{Bmatrix} J & J' & 1\\ 1 & 2 & J\end{Bmatrix}. \tag{6}$$

Since in the case of the alkali atoms there is a single external electron, the reduced matrix elements in these formulae may be expanded as follows:

$$|(nlj\|\,p\,\|n'l'j')|^2 = (2j+1)(2j'+1)\begin{Bmatrix} l & j & \frac{1}{2}\\ j' & l' & 1\end{Bmatrix} \cdot e^2\, l_> \left(\int_0^\infty R(nlj)\,r\,R(n'l'j')\,dr\right)^2, \tag{7}$$

where the ordinary notations for the quantum numbers n, l and j have been used, and $l_>$ means the greater of l and l'. From (5) and (7) the scalar polarizability of an S-state in an alkali atom is evaluated:

$$\alpha_0 = -\tfrac{2}{9}[\kappa(nS_{1/2},P_{1/2})+2\kappa(nS_{1/2},P_{3/2})] \tag{8}$$

where the terms κ are defined according to

$$\kappa(nL_J,L'_{J'}) = e^2\sum_{n'}\frac{\left(\int_0^\infty R(nlj)\,R(n'l'j')\,r\,dr\right)^2}{E(nL_J)-E(n'L'_{J'})}. \tag{9}$$

From (6) it follows that α_2 is identically zero in the first order of approximation when $J=1/2$. Using the terms κ we get in the same manner from Equations (5)–(7) for a $^2D_{3/2}$ state:

$$\alpha_0 = -\tfrac{2}{3}[\tfrac{1}{3}\kappa(nD_{3/2},P_{1/2}) +\tfrac{1}{15}\kappa(nD_{3/2},P_{3/2})+\tfrac{3}{5}\kappa(nD_{3/2},F_{5/2})] \tag{10}$$

and

$$\alpha_2 = \tfrac{2}{9}\kappa(nD_{3/2},P_{1/2})-\tfrac{8}{225}\kappa(nD_{3/2},P_{3/2}) +\tfrac{2}{25}\kappa(nD_{3/2},F_{5/2}). \tag{11}$$

The polarizability constants of a $^2D_{5/2}$ state are

$$\alpha_0 = -\tfrac{2}{3}[\tfrac{2}{5}\kappa(nD_{5/2},P_{3/2}) +\tfrac{1}{35}\kappa(nD_{5/2},F_{5/2})+\tfrac{4}{7}\kappa(nD_{5/2},F_{7/2})] \tag{12}$$

and

$$\alpha_2 = \tfrac{4}{15}[\kappa(nD_{5/2},P_{3/2})-\tfrac{4}{49}\kappa(nD_{5/2},F_{5/2}) +\tfrac{25}{49}\kappa(nD_{5/2},F_{7/2})]. \tag{13}$$

For states not too close to the ionization limit, the sum κ in (9) has in general one dominant term. By using the fractional contribution $k_{n'L'_{J'}}$ of this term,

$$e^2\frac{\left(\int_0^\infty R(nlj)\,R(n'l'j')\,r\,dr\right)^2}{E(nL_J)-E(n'L'_{J'})},$$

to the summations, Equation (9) may be written:

$$\kappa(nL_J, L'_{J'}) = \frac{e^2}{k_{n'L'_{J'}}} \frac{\left(\int_0^\infty R(nlj)R(n'l'j')r\,dr\right)^2}{E(nL_J) - E(n'L'_{J'})}. \quad (14)$$

It is then possible to determine the absorption oscillator strength $f_{nl\to n'l'}$ for the transition involving the mainly contributing state, from the values of α_0 and α_2 of the studied state. E.g. for a $P \leftrightarrow D$ transition we get

$$f_{nl\to n'l'} = (-1)^{l+1} \frac{120\pi^2 mc^2}{e^2}$$
$$\cdot \left(\tfrac{1}{5}\alpha_0(D_{3/2}) + \alpha_2(D_{3/2})\right) \left[\frac{4\lambda_{1/2,3/2}}{k_{1/2}} - \frac{\lambda_{3/2,3/2}}{k_{3/2}}\right]^{-1}$$
$$\cdot \sum_{jj'} \frac{1}{\lambda_{jj'}} (2j'+1) \begin{Bmatrix} j & 1 & j' \\ l' & 1/2 & l \end{Bmatrix},$$

where $\lambda_{1/2,3/2}$ and $\lambda_{3/2,3/2}$ are the wavelengths of the transitions $P_{1/2} \leftrightarrow D_{3/2}$ and $P_{3/2} \leftrightarrow D_{3/2}$, respectively, and $k_{1/2}$ and $k_{3/2}$ are the corresponding fractional contributions to the sums κ in (9). We have here dropped the j-dependence of the radial integral in (14). The summation is made for the different $j \to j'$ wavelengths of the studied transition. For the light alkali atoms the fractions k are close to unity and may be calculated with high accuracy using the Coulomb approximation according to Bates and Damgaard [9]. Oscillator strengths of some transitions in sodium have been estimated by Harvey et al. [6] using Stark-effect data. In the case of the heavy alkali atoms, such as cesium, the radial integrals have a j-dependence and the estimation of k is more complicated, due to an increasing spin-orbit coupling. The influence of the spin-orbit perturbation on the radiative properties is manifested, e.g. in the anomalous intensity ratios of doublet lines [10, 11]. In the sequence of S to P transitions in cesium, this ratio is changed from a value of 2 to values higher than 10 for some higher members in the sequence [12]. This is not according to the Coulomb approximation, giving values from 2 to 4. However, this approximation by no means takes the spin-orbit perturbations into full account. Thus, it is difficult to estimate k and give reliable values of the oscillator strength f.

3. Experimental Set-up

A schematic diagram of the apparatus used in the Stark-effect measurements is shown in Figure 1. A small oven placed in a vacuum chamber produced the beam of the alkali metal to be studied. The atoms in the beam were excited in a two-step process into a highly excited ^2S state or ^2D state. In the first step of the excitation process, the intermediate P state was populated by means of a powerful rf discharge lamp. The lamp cylinder, containing cesium or rubidium, was heated to approximately 130 °C and excited in the coil of a push-pull oscillator. The wavelengths of

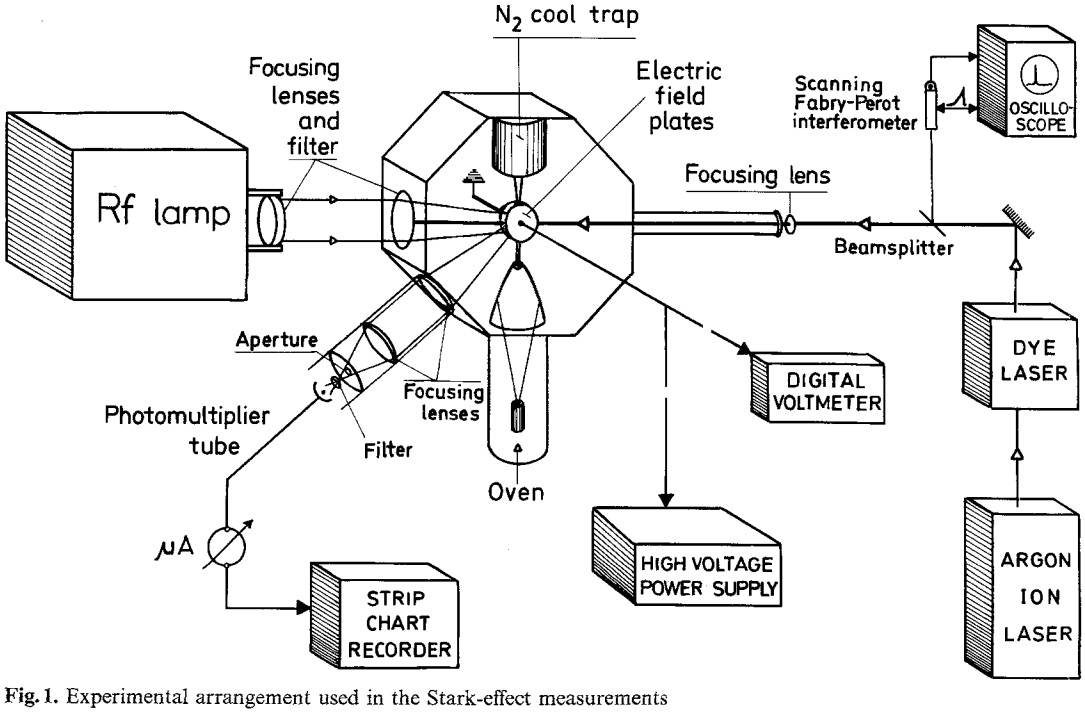

Fig. 1. Experimental arrangement used in the Stark-effect measurements

the excitation lines to the fine-structure levels of the first P-state are 8521 Å and 8943 Å in cesium. The corresponding wavelengths for rubidium are 7800 Å and 7948 Å. In the light beam of the cesium rf lamp a Schott RG 780 coloured glass filter, which removed all wavelengths below 7000 Å, was used. The rubidium rf lamp was utilized with a Schott RG 715 filter with no transmission of light below 6700 Å.

In the second step of the excitation, the atoms were transferred to a highly excited ^2S or ^2D state by the radiation of a CW tunable dye laser. The laser system used in these experiments was a Coherent Radiation Model 490, pumped by a CR-12 argon-ion laser. We used the dyes Rhodamine 110 and Coumarin 6 to cover the wavelength region 5200–6000 Å. By means of two quartz etalons, 10 mm and 0.5 mm thick, placed inside the laser cavity and tilted individually to the perpendicular plane of the cavity, all axial modes but one could be suppressed. The line-width of the laser output was about 75 MHz, due to jitter in the jet and the cavity. The single-mode frequency could be easily changed several GHz in steps of 313 (15) MHz, the mode spacing of the laser cavity, by further tilting the two etalons the same angle. The single-mode operation of the laser was controlled by a scanning Fabry-Pérot interferometer with a free spectral range of 1500 MHz, connected to an oscilloscope.

In order to reduce the Doppler width of the atomic absorption lines, the laser beam was incident perpendicularly to the moderately collimated atomic beam.

Over the interaction region a homogeneous electric field was generated by two 6 cm diameter electric field plates. The separation of the plates was 2.60 cm. Electric field strengths up to 7 kV/cm could be obtained.

The detection of fluorescent light in the cascade decay of the studied ^2S or ^2D state was made with an EMI 9558 BQ photomultiplier tube. In the measurements on cesium the decay of the $7\,^2P_{1/2,3/2}$ states to the ground state was studied and correspondingly, for rubidium the decay of the $6\,^2P_{1/2,3/2}$ states. The studied fluorescent light was selected for wavelength with interference filters at 458 nm and 421 nm, respectively. The interference filters were combined with different Schott coloured glass filters to further suppress the background light.

4. Measurements and Evaluations of Stark Parameters

Measurements of α_0 were performed for the 9 and $10\,^2S_{1/2}$ and the 7 and $8\,^2D_{3/2}$ levels of rubidium, and for the 12 and $13\,^2S_{1/2}$, the 9 and $10\,^2D_{3/2}$, and the 10 and $11\,^2D_{5/2}$ levels of cesium. We have earlier reported measurements for the 10 and $11\,^2S_{1/2}$ levels

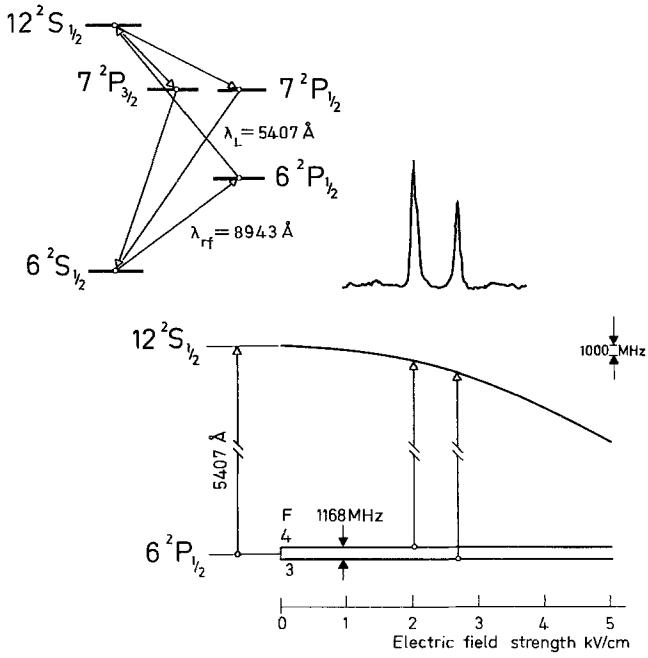

Fig. 2. Stark-effect measurement for the $12\,^2S_{1/2}$ state of ^{133}Cs. The hyperfine structure in the S-state does not resolve

and the $9\,^2D_{5/2}$ level of cesium [5]. The α_2 parameters of all these D-states have been measured earlier in our laboratory by level-crossing spectroscopy except for $11\,^2D_{5/2}$ in cesium [2, 3]. The α_2 value for this latter state was measured in this work.

In the experiments the energy levels were Stark-scanned by the application of an electric field. The levels were scanned till an excitation could occur for the set laser frequency. The electric field necessary for different transitions yielded information on the Stark-effect parameters. In the case of $J=1/2$ states, the α_2 parameter is identically zero in the first order approximation, as already noted. Therefore, the hyperfine components of such levels are equally shifted by the Stark effect. This case is illustrated by the $12\,^2S_{1/2}$-state of ^{133}Cs. Figure 2 shows the recording of the hyperfine components of the transition $6\,^2P_{1/2} \leftrightarrow 12\,^2S_{1/2}$ obtained when the electric field was scanned and the laser was running at a suitable single-mode frequency. The hyperfine structure in the $^2S_{1/2}$ state does not resolve. The recording was made by observing the fluorescent light emitted in the $7\,^2P_{3/2,1/2} \rightarrow 6\,^2S_{1/2}$ transition. By measuring the electric fields $\mathcal{E}_1$ and $\mathcal{E}_2$, necessary to achieve the resonance condition for the well separated hyperfine components, the difference in the α_0-value for the $12\,^2S_{1/2}$ and the intermediate $6\,^2P_{1/2}$ states can be calculated from Equation (1), as the separations of the hyperfine components of ^{133}Cs are known from the literature (see e.g. [3]).

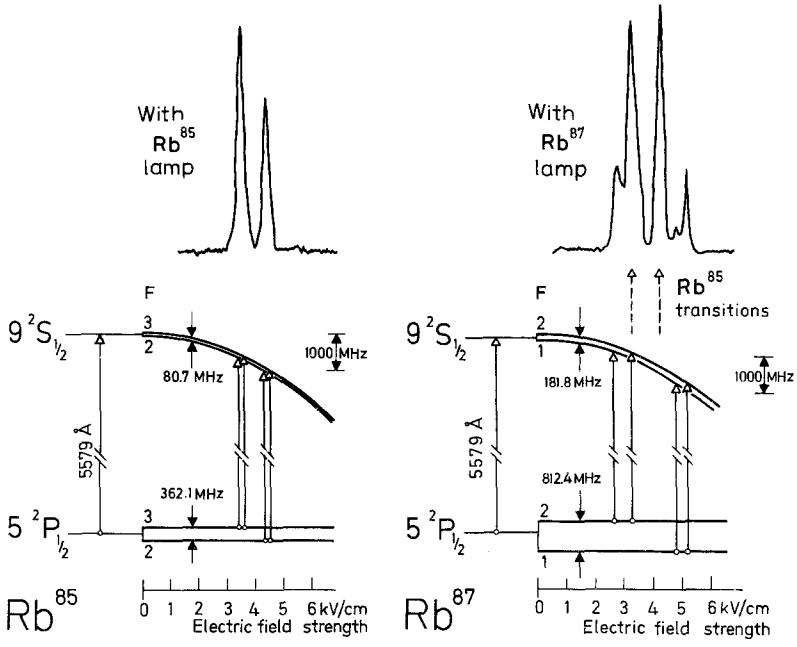

Fig. 3. Stark-scans for the $5\,^2P_{1/2} \rightarrow 9\,^2S_{1/2}$ transition in rubidium. The level schemes for both stable rubidium isotopes are shown. The individual isotopes could be enhanced by using separated isotopes in the rf lamp, used for populating the intermediate $5\,^2P_{1/2}$ state

A similar experiment for rubidium is shown in Figure 3, illustrating the scanning of the energy levels of the $9\,^2S_{1/2}$ state of rubidium. There are two rubidium isotopes, ^{85}Rb and ^{87}Rb. These have abundances of 72% and 28%, respectively, in the natural rubidium used in the atomic beam. These isotopes have different hyperfine structures as is illustrated in the figure. Further, there exists an isotope shift in the transition. This means, that the centres of gravity for the hyperfine components of the two isotopes do not coalesce. The excitation and detection scheme for the measurements is shown in Figure 4. In order to simplify the evaluation of the experiment we used the following procedure: By using enriched ^{85}Rb or ^{87}Rb in the lamp cylinder of the rf lamp, the population in the $5\,^2P_{1/2}$ state of one of the isotopes was enhanced. This implied that the relative strengths of the signal components for the isotopes were changed. Figure 3 shows recordings obtained using the two different isotope lamps. It can be noted that even with an ^{87}Rb rf lamp one can observe the transitions for ^{85}Rb. This is due to the partial overlap of the different isotope lines of the rf lamp caused by the Doppler broadening. Thus the $5\,^2P_{1/2}$ state in ^{85}Rb is populated to some extent. In the other case, with an ^{85}Rb rf lamp, the transitions of ^{87}Rb are not observed because of the smaller percentage of ^{87}Rb in the atomic beam. The hyperfine structure in the $9\,^2S_{1/2}$ level in ^{85}Rb is not resolved in our experiments as the splitting is too small, but for ^{87}Rb the upper state splitting can be seen. The evaluation of the Stark parameter is made in a similar way as for the previously described experiment in cesium. The necessary hyperfine-splitting constants are known from the literature [2]. For the isotope shift between the two rubidium isotopes we evaluated for the 5579 Å line $\Delta\sigma(87,85) = +76(20)$ MHz. This value is very close to the normal mass shift, +79 MHz [13].

Another way to obtain the same information on the Stark effect without using the hyperfine splittings, is to change the single-mode frequency of the laser beam in the measurements. The procedure is as follows: The electric field $\mathcal{E}_1$, necessary for one of the components of the transition to occur is measured. The single-mode frequency is then shifted by a certain number of discrete mode-hops, observed with the spectrum analyzer, whereupon the electric field $\mathcal{E}_2$,

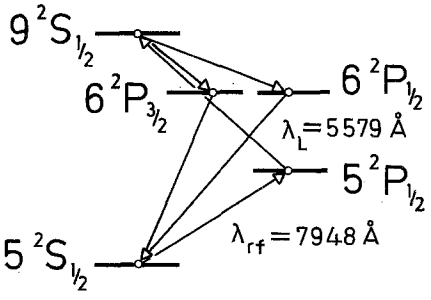

Fig. 4. Excitation and detection scheme used in the measurements, illustrated in Figure 3

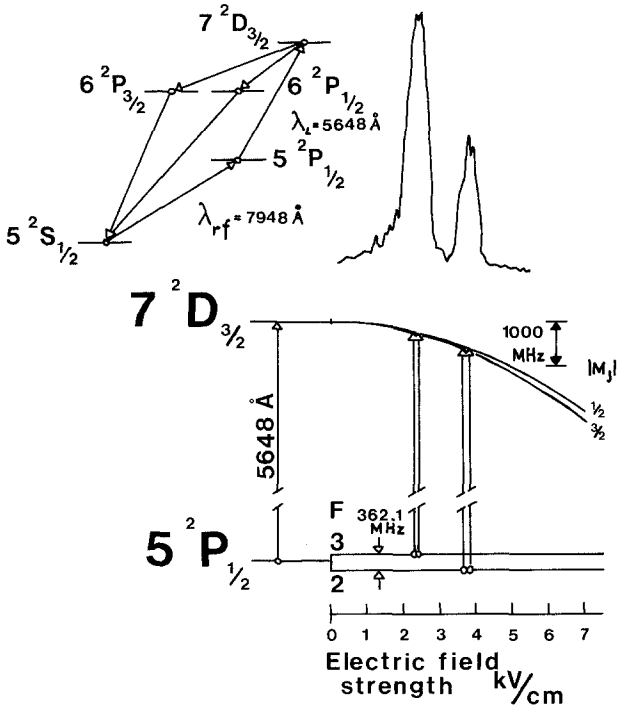

Fig. 5. Stark-effect measurement for the $7\,^2D_{3/2}$ state of rubidium. The structure is due to ^{85}Rb, as an rf lamp, containing only this isotope, was used

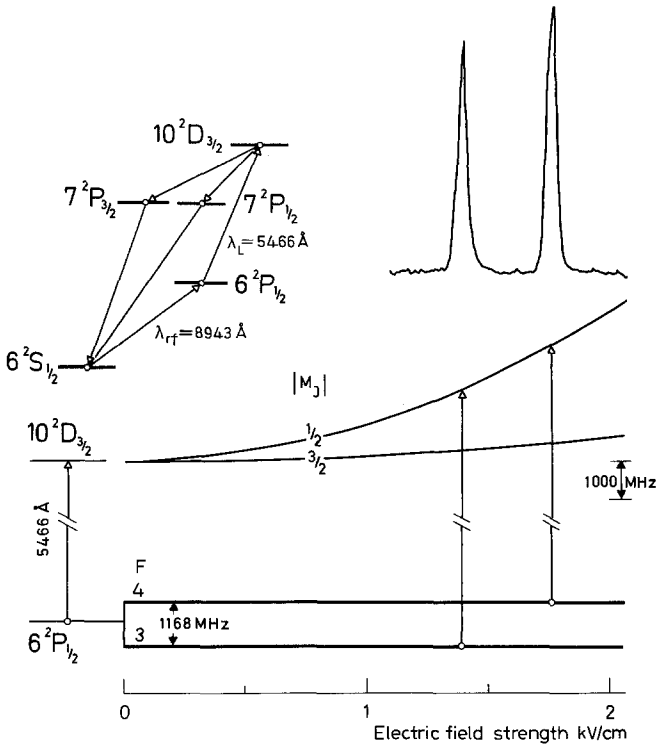

Fig. 6. Stark-scan for the $6\,^2P_{1/2}-10\,^2D_{3/2}$ transition in ^{133}Cs. As the α_2 parameter is previously known, the α_0 value can be evaluated from a curve like the one displayed in this figure

corresponding to the same hyperfine component and the new laser frequency, is measured. Using the readings $\mathcal{E}_1$ and $\mathcal{E}_2$ together with the known frequency shift, the difference between the α_0 parameters of the studied $^2S_{1/2}$ state and intermediate $^2P_{1/2}$ state can be obtained from Equation (1).

In cases where the scalar polarizability α_0 in states with tensor polarizability $\alpha_2 \neq 0$, are to be determined, the same type of measurements can be used if the α_2 value is known, again using (1). The α_2 values of all the studied states, except $11\,^2D_{5/2}$ in Cs, are known from Refs. [2, 3]. The hyperfine structure of the studied ^2D states is completely negligible compared to our resolution. Figure 5 shows as an example the splitting of the $7\,^2D_{3/2}$ state in ^{85}Rb due to the electric field. The level is split into two levels with different absolute values of m_J. In this case also the splitting due to α_2 is too small to be resolved at the electric field strengths used. The figure shows the curve obtained when the field was scanned and the laser was running in a single axial mode at a certain frequency.

The α_0 parameters in the ^2D states of ^{133}Cs were determined in still another way. Examples are given in Figures 6 and 7, showing the electric field dependence of the $10\,^2D_{3/2}$ and $10\,^2D_{5/2}$ levels of ^{133}Cs. The $10\,^2D_{3/2}$ level is scanned into two sublevels, each of them with a positive contribution to the energy. This is described by (1), from which we get the additional energy terms

$$-\tfrac{1}{2}(\alpha_0+\alpha_2)\mathcal{E}^2 \quad \text{for } |m_J|=3/2$$

and

$$-\tfrac{1}{2}(\alpha_0-\alpha_2)\mathcal{E}^2 \quad \text{for } |m_J|=1/2.$$

A recording of the fluorescence light emitted in the $7\,^2P_{1/2,\,3/2}\rightarrow 6\,^2S_{1/2}$ transition as the electric field was scanned and the laser was running at a suitable frequency, is also shown in the figure. The scanning and splitting of the $10\,^2D_{5/2}$ level of ^{133}Cs is displayed in Figure 7. In this case we get three sublevels, with the following contributions to the energy:

$$-\tfrac{1}{2}(\alpha_0+\alpha_2)\mathcal{E}^2 \quad \text{for } |m_J|=5/2,$$

$$-\tfrac{1}{2}(\alpha_0-\tfrac{1}{5}\alpha_2)\mathcal{E}^2 \quad \text{for } |m_J|=3/2$$

and

$$-\tfrac{1}{2}(\alpha_0-\tfrac{4}{5}\alpha_2)\mathcal{E}^2 \quad \text{for } |m_J|=1/2.$$

We have found the energy term of the $|m_J|=5/2$ level to be negative and the others to be positive. The upper part of Figure 7 shows an experimental curve obtained as the electric field was scanned and the laser frequency was somewhat higher than the

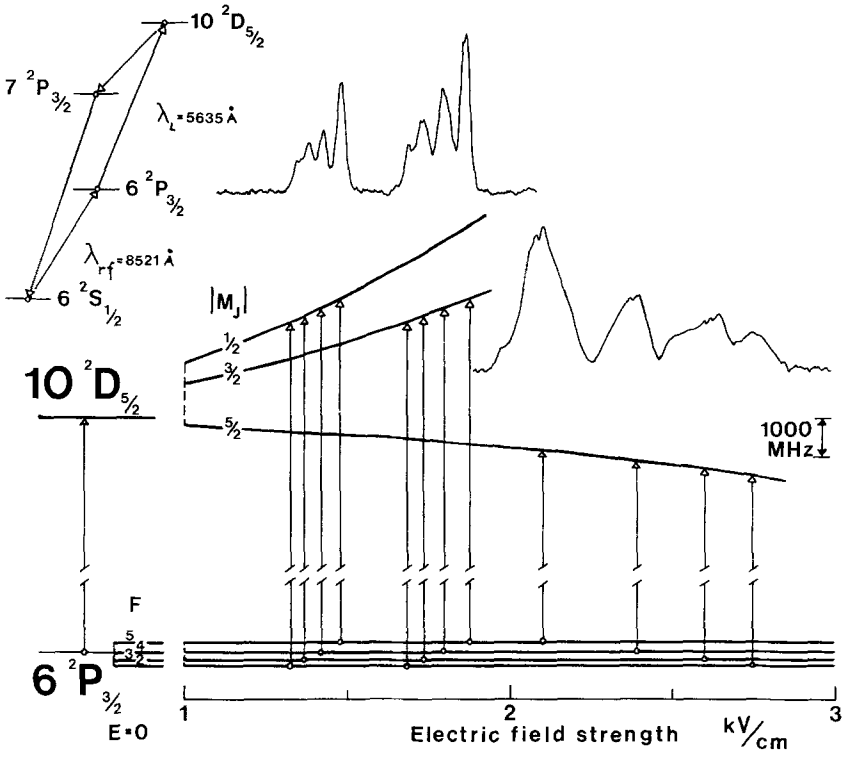

Fig. 7. Stark-scans for the $6\,^2P_{3/2}-10\,^2D_{5/2}$ transition in ^{133}Cs. Curves for the laser frequency set above and below the field-free resonance value are shown. The splittings between the sublevels of the $6\,^2P_{3/2}$ state are 151, 201, and 252 MHz

frequencies of the transitions studied in the absence of the electric field. Since the $|m_J|=5/2$ sublevel is scanned with a negative contribution to the energy it can not be reached with the same laser frequency, but requires a laser frequency somewhat lower than the transition frequency in the absence of the electric field. Such a recording is shown in the right part of Figure 7.

The measured electric field strengths $\mathcal{E}_1$ and $\mathcal{E}_2$, necessary to get contact with the sublevels $|m_J|=1/2$ and $|m_J|=3/2$ of a certain ^2D-state in ^{133}Cs, give us together with the known α_2 constant what is needed for the determination of α_0 according to the expressions given above.

In the state $11\,^2D_{5/2}$ of ^{133}Cs, where the α_2 constant had not earlier been determined, all three measuring methods, described above, were performed. By combining the method using the hyperfine splitting of the $^2P_{3/2}$-state with the last one described, and similarly combining the method of changing the laser frequency with the last method, both the α_0 and α_2 parameters of this state were determined. In Figure 8 a high-field measurement for the $11\,^2D_{5/2}$ state is shown. The hyperfine structure of the $6\,^2P_{3/2}$ state does not resolve as in Figure 7, due to the field-inhomogeniety broadening of the signal components. For most of the states studied in this work, two or three of the

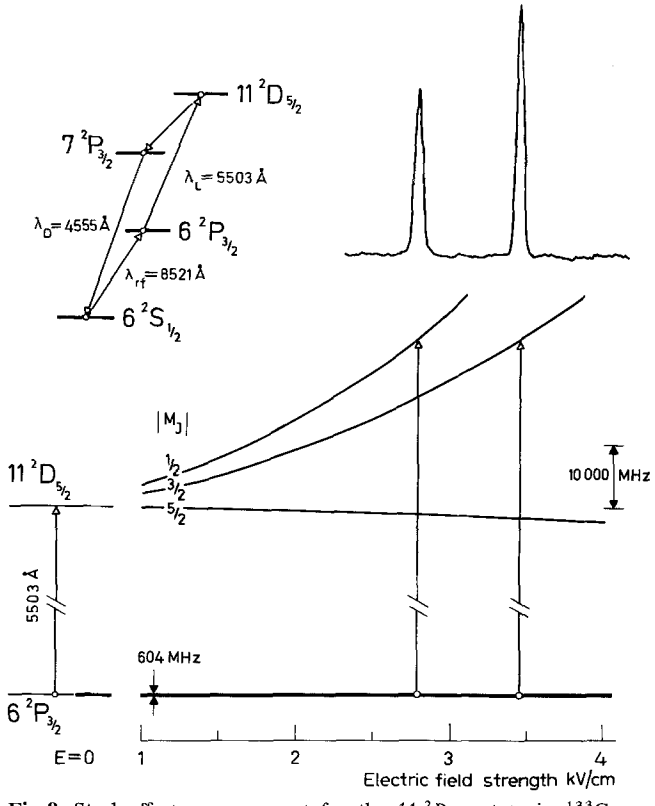

Fig. 8. Stark-effect measurement for the $11\,^2D_{5/2}$ state in ^{133}Cs. The P-state hyperfine structure does not resolve in this case because of the field-inhomogeniety broadening of the signal components present for large Stark shifts like the ones displayed

Table 1. Experimental values of polarizability constants obtained in this work

State	α_0 MHz/(kV/cm)^2	α_2 MHz/(kV/cm)^2
Cs $10\,^2S_{1/2}$	123(6)	
$11\,^2S_{1/2}$	322(16)	
$12\,^2S_{1/2}$	720(45)	
$13\,^2S_{1/2}$	1650(170)	
$9\,^2D_{3/2}$	− 360(30)	
$9\,^2D_{5/2}$	− 509(25)	
$10\,^2D_{3/2}$	−1150(170)	
$10\,^2D_{5/2}$	−1340(130)	
$11\,^2D_{5/2}$	−3790(350)	4010(400)
Rb $9\,^2S_{1/2}$	102(9)	
$10\,^2S_{1/2}$	280(25)	
$7\,^2D_{3/2}$	84(6)	
$8\,^2D_{3/2}$	211(18)	

mentioned methods were used for obtaining independent information. In order to ascribe α_0 values to the S and D levels studied in this work, we have applied a small correction for the intermediate P states to the values measured. The tensor polarizabilities of the intermediate $^2P_{3/2}$ states are extremely small and are therefore neglected. In cases where signal components overlap, we have used the theoretical intensities for calculating the "effective" positions. The results of the Stark-effect measurements are given in Table 1. Apart from the statistical noise, the electric-field and the mode-separation uncertainties determine the errors. Further, some of the measurements are influenced by the uncertainty in previously measured α_2-values.

5. Discussion

For all the studied states, theoretical calculations have been performed using the method of Bates and Damgaard [9]. In this method the radial integrals, determining the Stark-effect parameters, are calculated with the approximation of a Coulomb potential for the outer electron. However, the method is not wholly theoretical, as the experimentally determined energy levels are used in the calculations. Radial integrals between the studied level and levels up to $12F$ and $11P$ for Cs and Rb, respectively, have been taken into account in these calculations of the α_0 and α_2 parameters.

The scalar and tensor polarizabilities of Rb and Cs obtained in this work and those known from the literature are listed in Tables 2 and 3, together with the theoretical values. A fair agreement exists between the experimental and theoretical values.

For the D-states in the light alkali metals, there exist simple, approximate relationships between the Stark-effect parameters. This is due to the weak spin-orbit coupling in such states. From Equations (5), (6) and (7) we then obtain, dropping the j dependence of the radial integral in (7), and neglecting fine-structure splittings

$$\alpha_0(n^2D_{3/2}) = \alpha_0(n^2D_{5/2})$$

and

$$\tfrac{7}{10}\alpha_2(n^2D_{5/2}) = \alpha_2(n^2D_{3/2}).$$

In rubidium and cesium, however, the spin-orbit coupling is much larger causing a substantial fine-structure splitting and mixing of the states in a ^2L_J sequence [10–12, 14]. This leads to strong anomalies, e.g. in the doublet intensity ratios, as discussed in Section 2. Clearly, the assumptions leading to the simple relations given above are no longer valid. It is also found from the experimental values for Rb and Cs, given in Tables 2 and 3, that no simple relations exist. In view of this the Coulomb approximation values for the Stark interaction constants are in astonishingly good agreement with experiment.

We have already earlier pointed out certain difficul-

Table 2. Experimental and theoretical values of the Stark effect parameters for excited states in Rb

State	α_0 exp MHz/(kV/cm)^2	α_0 theor MHz/(kV/cm)^2	α_2 exp MHz/(kV/cm)^2	α_2 theor MHz/(kV/cm)^2
$9\,^2S_{1/2}$	102(9)	103		
$10\,^2S_{1/2}$	280(25)	271		
$5\,^2P_{3/2}$			−0.040(6)	
$6\,^2P_{3/2}$			−0.521(21)	
$7\,^2P_{3/2}$			−3.2(2)	
$6\,^2D_{3/2}$			−0.105(7)	−0.134
$6\,^2D_{5/2}$			0.94(5)	0.867
$7\,^2D_{3/2}$	84(6)	83.3	4.95(25)	4.67
$7\,^2D_{5/2}$			11.90(60)	11.2
$8\,^2D_{3/2}$	211(18)	233	27.0(1.4)	26.5
$8\,^2D_{5/2}$			56.9(3.0)	52.8
$9\,^2D_{5/2}$			180.3(9.0)	

Table 3. Experimental and theoretical values of the Stark-effect parameters for excited states in Cs

State	α_0 exp MHz/(kV/cm)^2	α_0 theor MHz/(kV/cm)^2	α_2 exp MHz/(kV/cm)^2	α_2 theor MHz/(kV/cm)^2
$10\,^2S_{1/2}$	123(6)	118		
$11\,^2S_{1/2}$	322(16)	309		
$12\,^2S_{1/2}$	720(45)	709		
$13\,^2S_{1/2}$	1650(170)	1490		
$6\,^2P_{3/2}$	0.398(60)	0.427	−0.065(10)	−0.059
$7\,^2P_{3/2}$		9.269	−1.077(43)	−0.172
$8\,^2P_{3/2}$		70.299	−7.6(3)	−7.523
$8\,^2D_{3/2}$			82.5(4.0)	83.9
$8\,^2D_{5/2}$			182(10)	168
$9\,^2D_{3/2}$	−360(30)	−348	313(15)	295
$9\,^2D_{5/2}$	−509(25)	−440	660(35)	592
$10\,^2D_{3/2}$	−1150(170)	−1052	840(40)	848
$10\,^2D_{5/2}$	−1340(130)	−1319	1770(90)	1705
$11\,^2D_{5/2}$	−3790(350)	−3383	4010(400)	4255
$13\,^2D_{5/2}$			$19(1)\times10^3$	20×10^3
$14\,^2D_{5/2}$			$37(2)\times10^3$	38×10^3
$15\,^2D_{5/2}$			$70(4)\times10^3$	70×10^3
$16\,^2D_{5/2}$			$120(6)\times10^3$	124×10^3
$17\,^2D_{5/2}$			$199(10)\times10^3$	213×10^3
$18\,^2D_{5/2}$			$323(16)\times10^3$	348×10^3

ties in deriving oscillator-strength values from the Stark effect parameters for the heavy alkali atoms. If we use the method outlined in the theoretical section we get, e.g. for the $12s\rightarrow12p$ and $11p\rightarrow10d$ transitions in cesium, the absorption oscillator strengths 4.22 and 1.47, respectively. The corresponding theoretical values are 3.67 and 1.57, respectively, calculated in the Coulomb approximation. However, these values are not quite reliable, as the strong spin-orbit interactions are not taken fully into account by the theoretical model used. A discussion of the Stark effect and the influences of the spin-orbit perturbations for the alkali metals will be given in a forthcoming paper.

The experimental technique used in this work may be applied in measurements, not only yielding the Stark interaction constants. Also small energy separations like isotope shifts can be measured, as was demonstrated. The method does not require a complex, continuously scanable single-mode laser, although such a laser has certain advantages in high-resolution laser spectroscopy.

The authors are very grateful to Professor I. Lindgren for valuable discussions and kind support. This work was financially supported by the Swedish Natural Science Research Council.

References

1. Belin, G., Holmgren, L., Lindgren, I., Svanberg, S.: Phys. Scr. **12**, 287 (1975)
2. Belin, G., Holmgren, L., Svanberg, S.: Phys. Scr. **13**, 351 (1976)
3. Belin, G., Holmgren, L., Svanberg, S.: Phys. Scr. **14**, 39 (1976)
4. Fabre, C., Haroche, S.: Opt. Commun. **15**, 254 (1975)
5. Fredriksson, K., Svanberg, S.: Phys. Lett. **53** A, 461 (1975)
6. Harvey, K.C., Hawkins, R.T., Meisel, G., Schawlow, A.L.: Phys. Rev. Lett. **34**, 1073 (1975)
7. Hawkins, R.T., Hill, W.T., Kowalski, F.V., Schawlow, A.L., Svanberg, S.: Phys. Rev. A, to appear
8. Khadjavi, A., Lurio, A., Happer, W.: Phys. Rev. **167**, 128 (1968)
9. Bates, D.R., Damgaard, A.: Phil. Trans. Roy. Soc. (London) **242**, 101 (1949)
10. Fermi, E.: Z. Physik **59**, 680 (1930)
11. zu Putlitz, G.: Comm. Atom. Molec. Phys. **1**, 51 (1969)
12. Fulop, G.F., Stroke, H.H.: Atomic Physics 3, New York: Plenum Press 1973
13. Kopfermann, H.: Nuclear Moments. New York: Academic Press 1958
14. Rydberg, S., Svanberg, S.: Phys. Scr. **5**, 209 (1972)

K. Fredriksson
S. Svanberg
Department of Physics
Chalmers University of Technology
Fack
S-40220 Göteborg 5
Sweden